Observation of Shear-Wave Mach Cones in a 2D Dusty-Plasma Crystal

V. Nosenko,* J. Goree,[†] and Z. W. Ma

Department of Physics and Astronomy, The University of Iowa, Iowa City, Iowa 52242

A. Piel

Institut für Experimentelle und Angewandte Physik, Christian-Albrechts Universität, Kiel, Germany

Mach cones composed of shear waves were observed experimentally in a two-dimensional screened-Coulomb crystal. Highly charged microspheres suspended in a plasma and interacting with a repulsive Yukawa potential arranged themselves in a triangular lattice with hexagonal symmetry. Mach cones were excited by applying a force from the radiation pressure of a moving laser beam. They had a single-cone structure, which is explained by the almost dispersionless character of shear waves. The cone's opening angle obeyed the Mach-cone–angle relation. Results are compared to a molecular-dynamics simulation.

A 2D crystalline lattice can vibrate in its plane with two kinds of sound waves, compressional and shear (i.e., transverse). In the shear wave, the particles are displaced from their equilibrium positions in a direction perpendicular to the wave vector $\mathbf{k}$. Shear waves obey a dispersion relation [1,2] that is different from that of the compressional waves in several ways: The shear wave has much less dispersion for long wavelengths $ka/\pi < 0.7$, where a is the interparticle spacing; it has a much slower sound speed $C = \omega/k$ for these long wavelengths; and it is unable to propagate in an ordinary liquid or gas. It can propagate in a strongly coupled liquid only if the wavelength is $\sim a$ [3–5]. The sound speed is determined by shear modulus and the bulk modulus, respectively, for the shear and compressional waves. Shear waves in a 2D screened-Coulomb crystal were recently observed experimentally [6].

When either of the waves are excited by a moving supersonic disturbance, the superposition of the waves creates a Mach cone, i.e., a V-shaped wake. Mach cones obey the Mach-cone–angle relation $\sin\mu = C/U$, where μ is the cone's opening angle, and U is the speed of the supersonic disturbance.

A dusty plasma is a suspension of micron-size particles in a plasma. The particles are highly charged, and, due to mutual repulsion, they arrange themselves in a regular pattern. Here we report results for a 2D triangular lattice with hexagonal symmetry, and a Yukawa interparticle potential. This lattice is characterized by the interparticle spacing a, shielding length λ_D, particle charge Q, and screening parameter $\kappa = a/\lambda_D$, which is typically ≈ 1 [7].

Mach cones in a 2D lattice were observed by Samsonov *et al.* [8,9], and Melzer *et al.* [10]. They were excited two ways: by the Coulomb force from charged particles moving spontaneously beneath a 2D lattice [8,9], and by the radiation force from a spot of focused laser light swept across the lattice at a speed U [10]. In these experiments, the Mach cones were composed of compressional waves.

Mach cones in solids are of interest in the fields of seismology and materials science. In seismology experiments, Mach cones were excited in a borehole [11]. Molecular dynamics (MD) simulations of a bcc tungsten crystal with a moving dislocation also exhibit a shear-wave Mach cone [12]. In a 2D Yukawa lattice, the existence of shear-wave Mach cones was predicted by Ma and Bhattacharjee [13].

Polymer microspheres were levitated in a plasma using an experimental setup (Fig. 1) similar to that of Refs. [8,10]. The primary difference compared to the setup of Ref. [10] is the laser excitation scheme, described below. A plasma was produced using a capacitively coupled
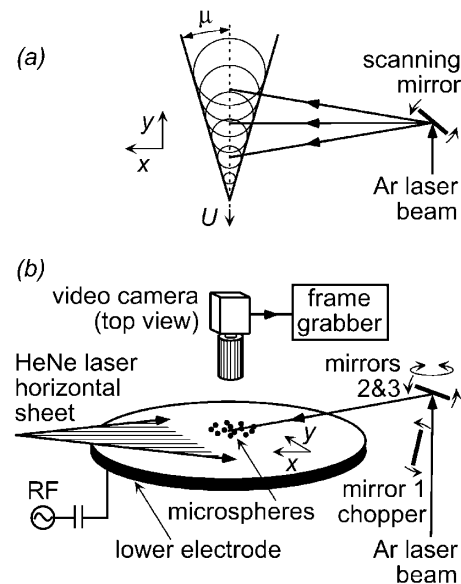

FIG. 1.   Experimental apparatus. (a) Mach cones are excited in a 2D lattice by applying the radiation force from a moving laser beam. (b) Polymer microspheres are levitated above the lower electrode in a capacitively coupled parallel-plate rf plasma. The particles settle in a single horizontal layer, arranged in a hexagonal lattice.

© 2002 The American Physical Society

parallel-plate rf discharge. We used 20 W of rf power at 13.56 MHz, with an amplitude of 84 V peak to peak. The self-bias voltage was −61 V. To permit propagation of shear waves, we used Ar at a low pressure of 15 mTorr, so that the Epstein drag was only $\nu = 2.7$ s^{-1} [14].

The lattice, which was triangular with hexagonal symmetry, consisted of a monolayer of particles suspended in the discharge. The particles were polymer microspheres with a diameter of 8.69 ± 0.17 μm, and mass density of 1.514 g/cm^3. The particles were viewed through the top window by a video camera, and they were illuminated by a horizontal He-Ne laser sheet. The 24×18 mm field of view included about 850 particles. The images were digitized with an 8-bit gray scale and a 640×480 pixel resolution. Particle coordinates and velocities were then calculated with subpixel spatial resolution [10], and the velocity field was then mapped onto a fixed grid. The lattice had a diameter of about 50 mm, an interparticle spacing of 762 ± 46 μm, and a pair correlation function $g(r)$ with many peaks and a translational order length of $4a$ to $18a$, indicating that the lattice was in the ordered state.

As a preliminary measurement, pulses of compressional and shear waves were launched in the lattice to measure the sound speeds using the methods of Refs. [6,15]. The pulses were excited by stimulating the particles with an Ar laser sheet that was chopped on and off. The sound speeds of the two modes were measured to be $C_L = 24.2 \pm 1.7$ mm/s and $C_T = 5.4 \pm 0.5$ mm/s, for the compressional and shear waves, respectively.

The ratio of the sound speeds, $C_L/C_T = 4.48 \pm 0.52$, is expected for our experimental conditions. This value corresponds to $\kappa = 1.19 \pm 0.28$, according to the theory of waves in a Yukawa crystal [2]. The particle charge is then calculated [2] to be $Q = -14\,100 \pm 1300e$. A variant of the resonance method of measuring particle charge [16] gave a lower value of $Q = -11\,000e$.

To observe shear-wave Mach cones, it was necessary to move the laser spot at a suitably low speed and to avoid excessively perturbing the lattice. Because of the shear wave's lower speed, and the Mach-cone–angle relation, the shear-wave Mach cones must have a significantly smaller opening angle μ. In Melzer's experiment [10], the region along the symmetry axis of the Mach cone's "V", corresponding to smaller opening angles, was highly perturbed, obscuring any small-angle features that might be present. To avoid perturbing this region, we used two variations of the laser excitation technique of Melzer et al. [10]. For the results we present first, the laser spot was moved in the direction perpendicular to the laser beam, i.e., perpendicular to the momentum imparted to particles by laser radiation. In this approach, the region corresponding to smaller opening angles was not perturbed. For the results appearing at the end of this Letter, the laser spot was moved in the direction of the laser beam, but with a reduced laser power so that the region behind the moving spot was not perturbed much. At its focus in

the vacuum chamber, the Ar laser beam had a power of 0.6 W, which we reduced to 0.12 W for lower scanning speeds. We recorded digital movies at 30 frames/s using the triggering scheme of Ref. [10].

The chief result of this experiment was the observation of a Mach cone composed of shear waves (Fig. 2), rather than compressional waves as in Fig. 2 of Ref. [8]. We moved the laser spot through the lattice with a speed $U = 11.2$ mm/s, which is about 2 times slower than the compressional wave sound speed, but still higher than the shear-wave sound speed. The shear-wave origin of this cone is demonstrated by four observations. First, the speed of scanning is too low, compared to C_L, to excite a compressional Mach cone. Second, the direction of the particle motion is parallel to the cone wings in Fig. 2(a) and, hence, perpendicular to the direction of wave propagation (which in turn is perpendicular to the cone's wings). This is different from compressional wave Mach cones where the particle displacement is perpendicular to the cone wings, and parallel to the wave propagation direction in Fig. 4(a) (below). Third, the feature appears prominently in a map of the vorticity, $|\nabla \times \mathbf{v}|$, where $\mathbf{v}$ is the particle velocity. This high "dynamic" vorticity of the Mach-cone feature in Fig. 2(b) demonstrates that the motion has significant shear. (Unlike a fluid, our medium is elastic, and it oscillates without breaking bonds after it is perturbed. Thus, the vorticity does not correspond to a vortex with circulation.) Fourth, a map of $\partial n/\partial t$, not shown here, where n is the particle number density, does not have any visible feature coinciding with the Mach cone. This type of map, also called a numerical Schlieren map [10], is effective for detecting compressive particle motion.

When we increased the scanning speed above the compressional wave sound speed C_L, we observed both the shear-wave Mach cones, with their smaller opening angles, and compressional wave Mach cones, with their larger angles. The latter were similar to the laser-excited Mach cones observed by Melzer et al. [10], except ours did not have a long disordered region behind the moving spot. In addition, a multiple-cone wake structure composed of compressional waves was observed. Similar wake structures were predicted by Dubin [17]. The compressional wakes have a multiple-cone structure arising from the wave dispersion. Our shear wakes, on the other hand, have only a single Mach cone, indicating that there is no significant dispersion [17]. This observation suggests that the wave numbers excited by our moving laser spot were in the range of $ka/\pi \leq 1.5$, which was identified by theory [1,2] as being dispersionless.

The Mach-cone–angle relation $\sin\mu = C/U$ is satisfied (Fig. 3) for both the shear and the compressional wave Mach cones, over a wide range of scanning speeds. The angle μ was measured from speed maps, which are not shown here, similar to those in Fig. 5 of Ref. [10]. The slope in Fig. 3 gives $C_T = 5.7 \pm 0.4$ mm/s and $C_L = 23.0 \pm 1.0$ mm/s. These values are consistent with the
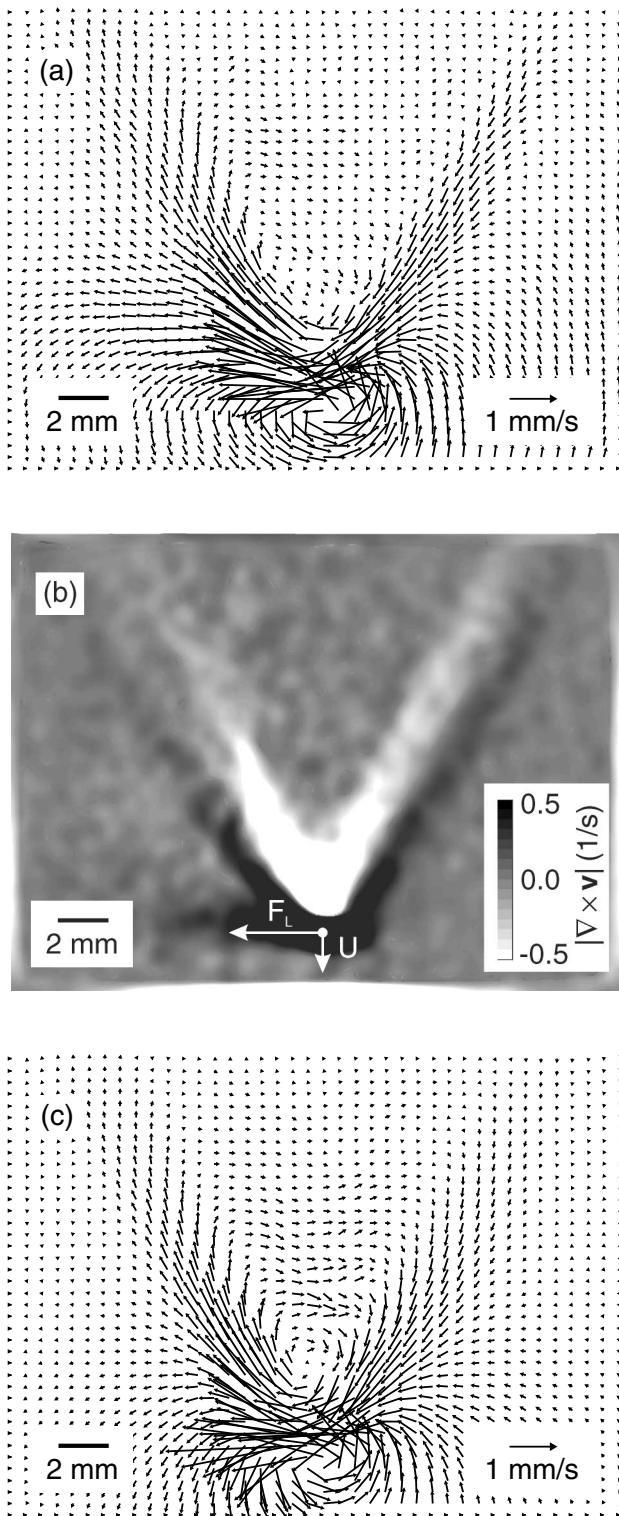
FIG. 2. Shear-wave Mach cone. The scanning speed is about 2 times lower than the compressional wave sound speed, but higher than the shear-wave sound speed. Maps are shown for (a) the particle velocity $\mathbf{v}$ and (b) to indicate shear motion, the vorticity $|\nabla \times \mathbf{v}|$. (c) Map of $\mathbf{v}$ from an MD simulation with a Yukawa interparticle potential. The parameters are similar to those for the corresponding experimental map in (a). The directions of the laser radiation force $\mathbf{F}_L$ and the laser spot scanning velocity $\mathbf{U}$ are indicated by arrows in (b).

preliminary measurements using compressional and shear-wave pulse propagation. The sound speed measurements made from the Mach cones are based on more experimental data. The values of the screening parameter and the particle charge, calculated from theory [2] using sound speeds from the Mach-cone angles, are $\kappa = 1.45 \pm 0.24$ and $Q = -15\,700 \pm 1100e$, respectively.

We performed a 2D MD simulation using experimental parameters similar to those of Figs. 2(a) and 2(b). The particle equation of motion $md^2\mathbf{r}/dt^2 = -Q\nabla\phi - m\nu d\mathbf{r}/dt + \mathbf{F}_L$ was integrated for 5000 particles. The electric potential ϕ consisted of a harmonic potential for the external radial confinement $-k\rho^2/2$ plus a binary interparticle repulsion, assuming a Yukawa model. Here ρ is the distance from the central axis. We used the parameters $Q = -15\,700e$, $\lambda_D = 526$ μm, $m = 5.2 \times 10^{-13}$ kg, and $\nu = 2.7$ s^{-1} for Epstein drag. We chose $k = 2.4 \times 10^{-13}$ kg/s^2 to obtain a lattice with a particle separation of 762 μm. After the particles formed a crystal, we introduced a moving localized force $\mathbf{F}_L$ to model the force due to the moving laser spot. The force had an elliptical Gaussian profile, as in Ref. [10]: $\mathbf{F}_L = f_0 \exp(-x^2/b_x^2) \times \exp[-(y - Ut)^2/b_y^2]\mathbf{x}$, with $b_y = 0.26$ mm, $b_x = b_y/\sin 10° = 1.48$ mm, and $f_0 = 7.8 \times 10^{-14}$ N. The laser spot speed was $U = 11.2$ mm/s.

Simulation results for the particle velocity are shown in Fig. 2(c), which is similar to the experimental velocity map in Fig. 2(a). Both the experiment and the simulation reveal shear-wave Mach cones with a single-cone structure. The cones have nearly the same opening angle $\mu = 32°$. The experiment and simulation differ slightly in the particle speed between the Mach cone's wings, and the asymmetry of the two wings. A possible reason for these differences is a slow rotation of the plasma crystal in the experiment.
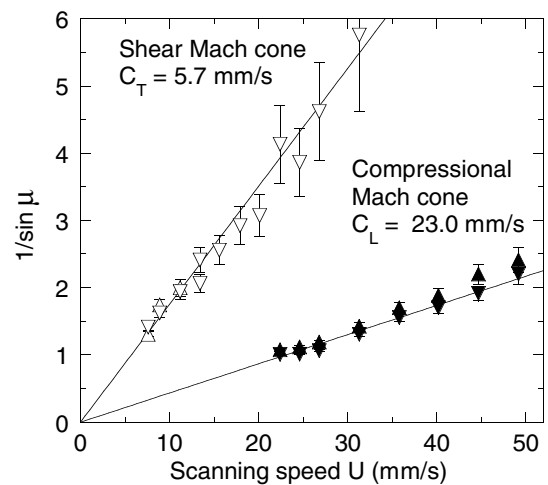

FIG. 3. Test of the Mach-cone–angle relation $\sin\mu = c/U$, where μ is the cone's opening angle, U is the speed of the supersonic disturbance, and c is the sound speed, for shear and compressional Mach cones. Here, μ is measured separately at the laser excitation side $\triangle$, and at the opposite side $\triangledown$.
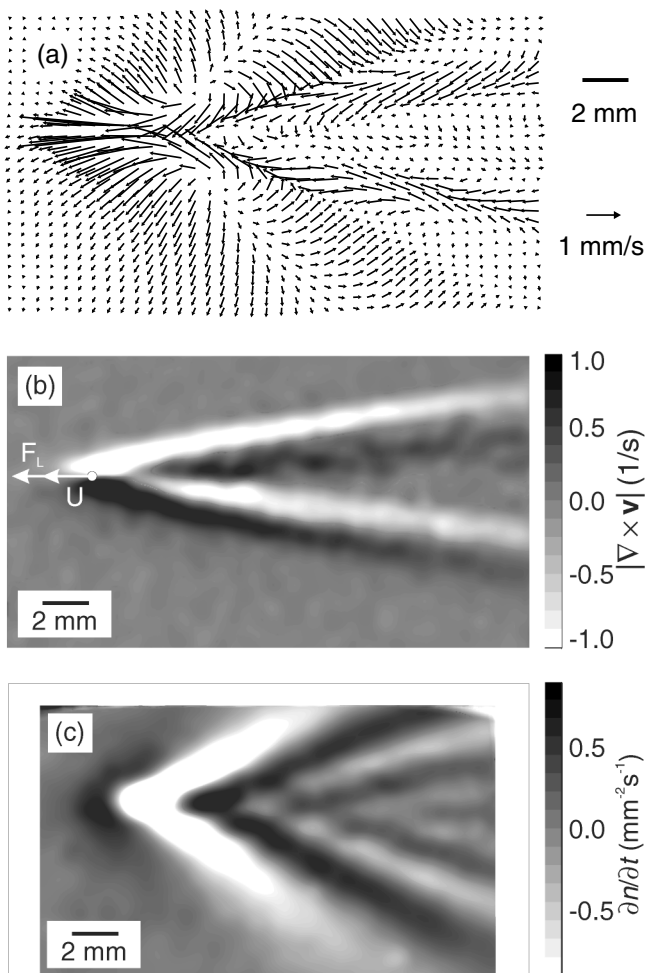
FIG. 4. Shear-wave and compressional wave Mach cones excited simultaneously. The laser scanning speed is higher than both C_L and C_T. Maps are shown for (a) particle velocity $\mathbf{v}$, (b) vorticity $|\nabla \times \mathbf{v}|$, and (c) $\partial n/\partial t$, where n is the particle number density. The directions of the laser radiation force $\mathbf{F}_L$ and the laser spot scanning velocity $\mathbf{U}$ are indicated by arrows in (b).

A second approach of exciting both compressional and shear-wave Mach cones simultaneously is to sweep the laser spot in the direction of the laser beam, as in Ref. [10], at a reduced laser power so that the region behind the moving spot is not perturbed by defect generation. We used this method in a separate experiment. The laser beam, which was reduced in power to 0.24 W, was swept through the lattice with a speed higher than both the compressional and the shear-wave sound speeds. As with the other approach described above, this yielded both shear and compressional wave Mach cones, and a multiple-cone compressional wake (Fig. 4). Note that the numerical Schlieren map, Fig. 4(c), reveals clearly the compres-

sional features of the Mach cone and multiple-cone wake, whereas the vorticity map emphasizes the shear-wave Mach cone [Fig. 4(b)]. When we increased the excitation laser power to 0.6 W and the rf power to 30 W, the shear Mach cone disappeared, replaced by a disordered region behind the moving spot, as in Ref. [10].

In summary, shear-wave Mach cones were observed experimentally in a 2D screened Coulomb crystal. To excite them, it was crucial to avoid excessively perturbing the lattice. Unlike compressional wave Mach cones, they have a single-cone structure, which we attribute to the almost dispersionless character of shear waves at long wavelengths. They obey the Mach-cone–angle relation, yielding a sound speed of shear waves of 5.7 mm/s, which is consistent with separate observations of shear-wave pulse propagation.

Note added.— New TEM measurements of our particles yielded a mean diameter of 8.09 μm, which is 7% smaller than the manufacturer's specification. Using this value, the corrected values of other parameters are $m = 4.2 \times 10^{-13}$ kg, $Q = -14\,100e$ (as given by the Mach-cone-angle relation method), and drag $\nu = 2.9$ s^{-1}.

*Electronic address:
†Electronic address:

[1] F. M. Peeters and X. Wu, Phys. Rev. A **35**, 3109 (1987).
[2] X. Wang, A. Bhattacharjee, and S. Hu, Phys. Rev. Lett. **86**, 2569 (2001).
[3] P. K. Kaw and A. Sen, Phys. Plasmas **5**, 3552 (1998).
[4] G. Kalman, M. Rosenberg, and H. E. DeWitt, Phys. Rev. Lett. **84**, 6030 (2000).
[5] H. Ohta and S. Hamaguchi, Phys. Rev. Lett. **84**, 6026 (2000).
[6] S. Nunomura, D. Samsonov, and J. Goree, Phys. Rev. Lett. **84**, 5141 (2000).
[7] A. Homann *et al.,* Phys. Rev. E **56**, 7138 (1997).
[8] D. Samsonov *et al.,* Phys. Rev. Lett. **83**, 3649 (1999).
[9] D. Samsonov *et al.,* Phys. Rev. E **61**, 5557 (2000).
[10] A. Melzer *et al.,* Phys. Rev. E **62**, 4162 (2000).
[11] N. Cheng *et al.,* Geophys. Prospect. **42**, 303 (1994).
[12] P. Gumbsch and H. Gao, Science **283**, 965 (1999).
[13] Z. W. Ma and A. Bhattacharjee (to be published).
[14] P. Epstein, Phys. Rev. **23**, 710 (1924).
[15] V. Nosenko, S. Nunomura, and J. Goree (unpublished).
[16] Th. Trottenberg, A. Melzer, and A. Piel, Plasma Sources Sci. Technol. **4**, 450 (1995).
[17] D. H. E. Dubin, Phys. Plasmas **7**, 3895 (2000).